

Automation of the Silk Spinning Process by the Creation of an Electronic Control System

***Benjamin Leaf[1], *Daniela Chavarría Umaña[2], *Christian Henning[2], Bradley Hoffmann[1], Amanda E. Brooks[3]**

[1]College of Mechanical Engineering
[2]College of Electrical Engineering
[3]College of Pharmaceutical Science
North Dakota State University, Fargo, ND 58105

* These authors contributed equally to this work

ABSTRACT

Spider silk has been the focus of study in many scientific disciplines during recent years due to the desirability of its versatile mechanical properties. Previous studies reported the fabrication of a biomimetic silk-spinning device to create artificial silk fibers using a combination of protein concentration, ionic gradients, and mechanical shear to mimic the natural silk spinning process of the Golden Orb Weaver spider (*Nephila clavipes*). Despite improvements, the current spinning device is not ideal as it utilizes syringes and tube fittings to apply the necessary spinning elements with a single controlled flow rate. This methodology as well as human error and interaction can lead to asymmetric fluid flow, causing inconsistency and undesirable qualities in the fibers collected from the device. The objective of this study was to create an electronic control system to monitor fluid flow and precisely control all elements of the spinning process. In this study calibration of the electronic control system was conducted through three spinning iterations. A calibrating trend line was derived from the combined tests to correlate the spinning fluid flow rates to diameter outputs. Iteration test 1 flow rates yielded 15 μm fiber diameter. Test 2 and 3 yielded 45 μm and 47 μm fiber diameter respectively. The calibration curve enabled offset values for the continued spinning system. Providing an autonomous control system with integrated monitoring will allow the resulting fiber characteristics to be correlated with specific spinning elements and leading to far more consistent and efficient fiber creation, while minimizing the human element of the process.

Keywords: Silk spinning, biomimetics, biomaterials, silkworm silk, spider silk

INTRODUCTION

Natural silks, such as those produced by spiders, are a fascinating material combining remarkable mechanical properties with low density and biodegradability [1]–[3]. Major ampullate spider silk's unsurpassed toughness is due to a unique combination of high tensile strength and elasticity, a product of both its protein structure and it spinning conditions. Of the natural spinning systems, those of the spider's major ampullate glands (dragline silk) are particularly complex, contradicting traditional, simplified spinning techniques. Dragline silk proteins are predominantly synthesized in specialized protrusions of the glands called the tail [4]. The proteins are subsequently gathered and stored in a gland sac, the so-called ampulla. During spinning, the material is passively transported through a duct that is approximately three times as long as would be required for it to connect the exit of the gland to the spinneret [5]. The conversion of the liquid material into solid fiber occurs at the end of the duct and is controlled by a biological valve, where fiber formation is facilitated via increased shear forces [6].

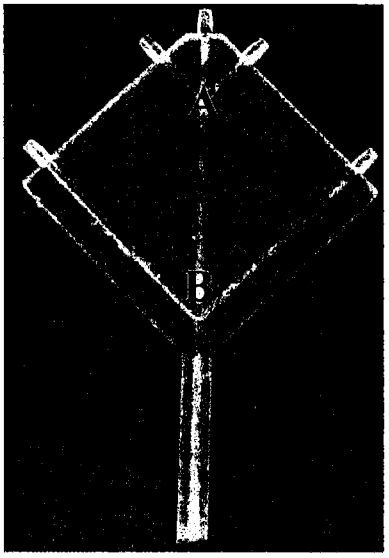

Figure 1: The microfluidic device note that the channels have a square geometry. The side channels meet the center channel at an optimum 45-degree angle.

To recapitulate the shear thinning forces prevalent in the tapering third region of the gland and the biological valve, a custom control system capable of producing fluid flow gradients via hydrodynamic focusing is necessary [6]. Artificially spun spider silks could indeed become an appealing alternative fiber when compared to other low-tech material alternatives such as nylon or cotton (which are cheap, but environmentally costly) or hi-tech materials, such as Kevlar, if they could be manufactured economically and consistently with a quantity and quality using environmentally friendly production methods [7].

A silk spinning microfluidic device has been previously investigated using rapid prototyping and 3D printing (Figure 1) [8]. This device allows the silk proteins to interact in a way that mimics the natural process of the golden orb weaver.

In the current design, fluids are injected into the microfluidic device by a syringe pump, which provides equal flow rates to all five inlets of the device. This setup is not ideal as it does not allow for changing the velocity in the different channels of the device, meaning mechanical shear due to fluid flow cannot be changed. As an initial attempt to circumvent this problem, the use of peristaltic pumps to apply fluid to the final channels of the device proved that varying the shear by changing the velocity will create fibers with differing properties [8]. This study improves the microfluidic-spinning device by integrating a customizable complex control system for spinning silk.

METHODS

The system was controlled using a Raspberry Pi microcomputer, incorporating a system of five peristaltic pumps to replace the 10 channel syringe pump entirely. This setup allowed for complete control over the spinning process, including varying the shear forces in the microfluidic device and controlling overall flow rate to speed up or slow down fiber production and alter the fiber properties.

Due to its availability and quantity, initial testing involved spinning silkworm silk produced by the silkworm (*Bombyx mori.*). Silk spin dope was prepped by degumming the silkworm silk at 100°C in an 0.5% wt/vol solution sodium carbonate for 60 min to remove the outer sercin protein coating. The silk was then rinsed with distilled water to remove excess sercin protein. The degummed silk was allowed to air dry for 24 hours. After air drying, degummed silk was directly dissolved in a 8% wt/vol calcium chloride/formic acid solution to produce an 8% wt/vol silk spin dope. The silk spin dope was then injected into the center channel while the side channels provide fluid flow gradients to the main channel spin dope.

The completed device consisted of a Raspberry Pi controller with three motor HATs to run the pumps. The code allowed pumps 4 and 5 to be run at a separate speed from 1, 2, and 3 to create

fluid shear in the second channel intersection through hydrodynamic focusing. The experiment consisted of pump 1 injecting the silk proteins into the center channel at the same rate that pumps 2 and 3 injected distilled water into the first set of side channels. Pumps 4 and 5 injected distilled water at a faster rate into the second set of side channels for hydrodynamic focusing (Figure 2). Pump 1 draws from the silk solution pictured at the top-center of the image, and pumps 2-5 draw from their respective DI water beakers. The device outlet is submerged in DI water to collect the fibers during the spinning process.

RESULTS

The junctions within the device are especially important, as the fluid interaction here creates a shear force, which aligns the silk proteins, facilitates secondary structure formation, and gives shape to the fibers. The level of shear experienced by the fluid had a significant contribution to the resulting diameter of the silk and its subsequent tensile strength. Higher shear creates thinner fibers, which show increased tensile strength when subjected to testing. In order to apply the final solution (channels 4 and 5) at a different rate from the proteins and ionic gradient (channels 1-3), the system must run the pumps at different speeds. These speeds correspond to the desired flow rates in the microfluidic device. Previous experiments provided the rates needed for different fiber diameters and these were used to determine pump flow rates for the new device. Velocity V was converted to flow rate Q by way of the area A of the microfluidic chip,

$$Q = AV. \tag{1}$$

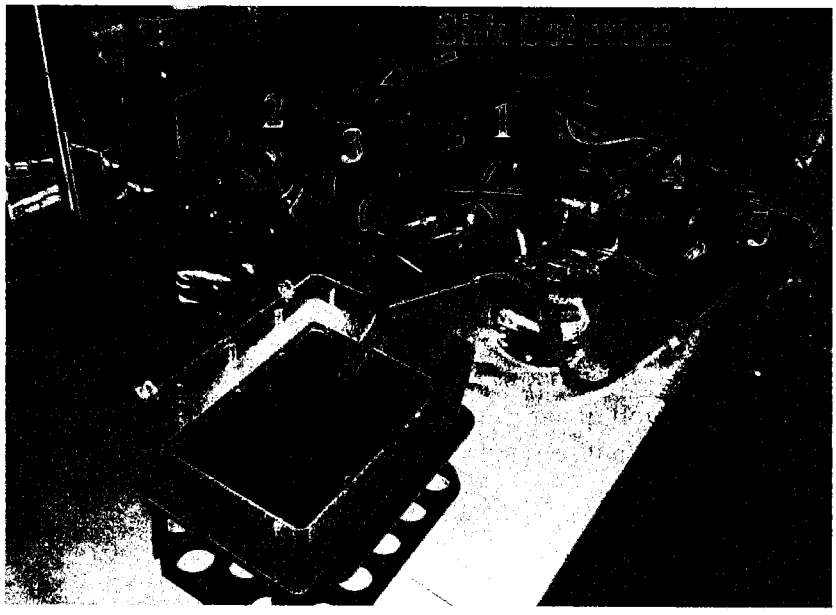

Figure 2: Experimental setup

The area of the chip was 2.25 mm^2. Thus for a velocity of 7.407 mm/s, Equation 1 provided a flow rate of 1 mL/min. For a velocity of 14.815 mm/s, the corresponding flow rate was 2 mL/min. Therefore, the controller input value needs to be determined for each flow rate to ensure accurate fiber creation. These rates were determined experimentally by measuring the amount of water moved by each pump individually in 30 seconds. A range of input values from 4 to 90 in the code were used for this purpose. A logarithmic regression was fit to the data to give the equation,

$$Q = 0.4422ln(Input) + 0.5546. \quad (2)$$

Where Q is the resultant flow rate corresponding to the input value. Equation 2 was used to determine the inputs needed for each experiment performed with the device. While testing the motors, microsteps were deemed ineffective due to the extremely small maximum flow rate. Additionally, interleaved steps and single steps did not turn the motors consistently, producing undesirable results. Thus, double stepping was chosen for fiber creation to provide consistent motor rotation while operating multiple speeds at once.

The first test was run at 1.1 mL/min for pumps 1-3 and 1.5 mL/min for pumps 4 and 5. This gradually produced a ball of fibers at the outlet of the device, and three were drawn from the device before the slow rate caused the channel to clog with hardening fluid in the outlet. This stoppage caused backflow in the DI water tubes as the higher pressure from the viscous protein solution caused a positive pressure gradient in the microfluidic chip. The next iteration replicates were performed with pumps 1-3 at 1.5 mL/min and pump 4 and 5 at 2.1 mL/min. Even though these conditions also seemed to create a ball of fiber at the outlet the additional fluid flow did not allow the ball to clog the channel while the pumps were running. Unfortunately, although one fiber was able to be drawn directly out of the collecting bath, the faster rate of fiber formation led to the fibers becoming entangled in the bath, limiting the number of fiber able to be tested. The fiber entanglement seemed to be strong and brittle, which may have caused fibers drawn from the entanglement to break quickly during pulling. Once the pumps were shut off, the pressure gradient again caused the silk solution to back fill and subsequently clog the water tubes within minutes.

The final iteration was run at 1.3 mL/min for pumps 1-3 and 1.8 mL/min for pups 4 and 5. One fiber was hand drawn from the device immediately upon startup, but again the fibers became entangled, and it became impossible to draw out additional fibers. Backflow once again caused silk to precipitate and condense in the water tubes, leading to cession of flow.

Only one fiber could be pulled with each iteration of the spinning system, leading to only preliminary results. However, one consistent observation through all three tests was the behavior of the fluid while decoupling the

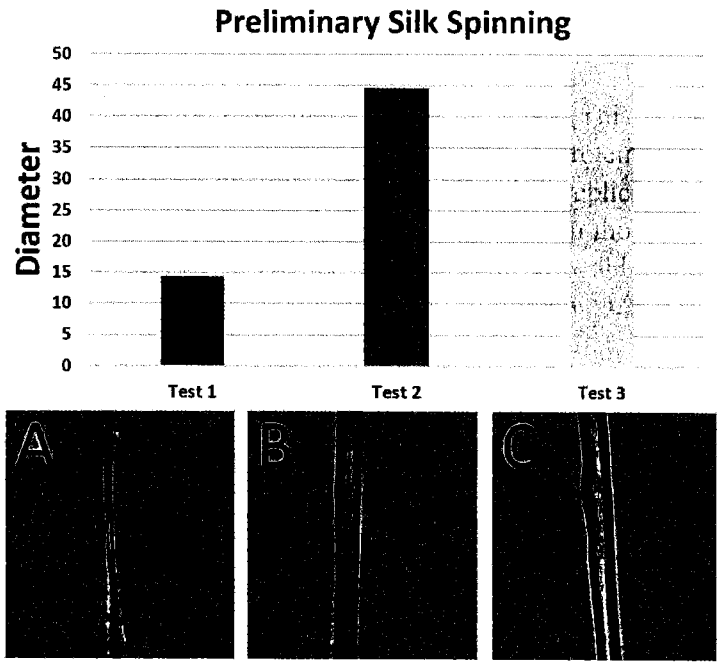

Figure 4: Fiber diameters from the three spinning tests have been collected. Test 1 fiber = 15μm **A**. Test 2 fiber = 45μm **B**. Test 3 fiber = 47μm **C**.

tubes from the microfluidic chip. Whenever the tube feeding the silk spin dope into the device was removed, the positive pressure in the four water tubes caused all excess silk fluid to run out of the inlet, and many fibers were observed. Fiber formation at this stage of the experiment was likely due to the higher pressure inside the device and the speed at which the proteins were expelled backwards out of the chip. Nevertheless, the development of fibers through each test allowed insight into the controlled fluid stream within the device. Preliminary fiber geometry was analyzed for fibers from each test (Figure 4). Fibers collected through controlling and fluidic focusing have shown to reduce fiber diameter [8]. This technique will continue to drive the control system design.

DISCUSSION

The successful integration of individual flow rates within the 3D printed chip style device allows improved control of the silk spinning process. Changing the spinning to variable rates instigates the use of fluid focusing, which provides fluid shear to "snap" the proteins in place and create a fiber. Controlling the shear allows the device to control fiber formation, leading to a complete system that can manipulate fiber output. The control system is built upon an existing silk spinning apparatus, leading to the continued advancement of microfluidic biomimetic spinning [8], [9]. The natural spinning process is an elaborate system that has been optimized through millions of years of evolution. Thus if the ultimate goal is to precisely mimic the fiber, utilizing the microfluidic device, the biochemical interactions of pH and ionic gradients found in the spinning gland must also be incorporated [10], [11]. Despite the fact that fluid flow gradients are the only piece of the puzzle that has been investigated so far, preliminary data reveals fiber diameters have been altered.

Through individual controlled peristaltic pumps it is now possible to isolate and investigate the impact of both pH and ionic gradients at the intersections of the device. In spite of the new challenges that arose during the course of these experiments, this study was able to conclude that there is a need for improved fiber collection. Improving the outlet draw ratio will enable smooth collection of uniform fiber output.

CONCLUSION

The secrets behind the strength of spider and silkworm silk will continue to leave an air of mystery as researchers strive to reproduce their unique and complex spinning systems. Through the work detailed in this manuscript, it was shown that it is possible to improve an already existing spinning system to initiate fluidic gradients, which aid in the synthetic spinning process to provide individual control of each channel and hence facilitate physical fiber formation and control fiber output geometry.

Observations in this study have allowed identification of future works that will prove vital to biomimicry of the natural silk process, including 1) improved silk collection, 2) introduction of pH and ionic components, and 3) alteration of the silk proteins to include spider silk proteins.

ACKNOWLEDGMENTS

This research was made possible through Discovery Based Learning at NDSU and with funding to Dr. Amanda Brooks lab from the National Science Foundation (grant number 1746111).

REFERENCES

[1] M. Lee, J. Kwon, and S. Na, "Mechanical behavior comparison of spider and silkworm silks using molecular dynamics at atomic scale," *Phys Chem Chem Phys*, vol. 18, no. 6, pp. 4814–4821, 2016.

[2] G. Fang *et al.*, "Insights into Silk Formation Process: Correlation of Mechanical Properties and Structural Evolution during Artificial Spinning of Silk Fibers," *ACS Biomater. Sci. Eng.*, vol. 2, no. 11, pp. 1992–2000, Nov. 2016.

[3] K. N. Kim *et al.*, "Silk fibroin-based biodegradable piezoelectric composite nanogenerators using lead-free ferroelectric nanoparticles," *Nano Energy*, vol. 14, pp. 87–94, May 2015.

[4] M. Andersson, J. Johansson, and A. Rising, "Silk Spinning in Silkworms and Spiders," *Int. J. Mol. Sci.*, vol. 17, no. 8, p. 1290, Aug. 2016.

[5] A. Rising and J. Johansson, "Toward spinning artificial spider silk," *Nat. Chem. Biol.*, vol. 11, no. 5, pp. 309–315, Apr. 2015.

[6] D. N. Breslauer, L. P. Lee, and S. J. Muller, "Simulation of Flow in the Silk Gland," *Biomacromolecules*, vol. 10, no. 1, pp. 49–57, Jan. 2009.

[7] D. U. Shah, D. Porter, and F. Vollrath, "Opportunities for silk textiles in reinforced biocomposites: Studying through-thickness compaction behaviour," *Compos. Part Appl. Sci. Manuf.*, vol. 62, pp. 1–10, Jul. 2014.

[8] B. Hoffmann, C. Gruat-Henry, P. Mulinti, L. Jiang, B. Brooks, and A. Brooks, "Development of a Complex Control System for Multiple Fluid Flow Gradients," *Biomed. Sci. Instrum.*, vol. 53, Apr. 2017.

[9] B. Hoffmann, A. Nodland, C. Gruat-Henry, and A. Brooks, "Using Engineering To Unravel The Mystery of Spider Silk Fiber Formation," *Biomed. Sci. Instrum.*, vol. 52, 2016.

[10] G. Askarieh *et al.*, "Self-assembly of spider silk proteins is controlled by a pH-sensitive relay," *Nature*, vol. 465, no. 7295, pp. 236–238, May 2010.

[11] W. A. Gaines, M. G. Sehorn, and W. R. Marcotte, "Spidroin N-terminal domain promotes a pH-dependent association of silk proteins during self-assembly," *J. Biol. Chem.*, vol. 285, no. 52, pp. 40745–40753, Dec. 2010.